Science Advances
AAAS

advances.sciencemag.org/cgi/content/full/6/47/eabd0276/DC1

Supplementary Materials for

PPM1G restricts innate immune signaling mediated by STING and MAVS and is hijacked by KSHV for immune evasion

Kuai Yu, Huabin Tian, Hongyu Deng*

*Corresponding author. Email: hydeng@moon.ibp.ac.cn

Published 20 November 2020, *Sci. Adv.* **6**, eabd0276 (2020)
DOI: 10.1126/sciadv.abd0276

This PDF file includes:

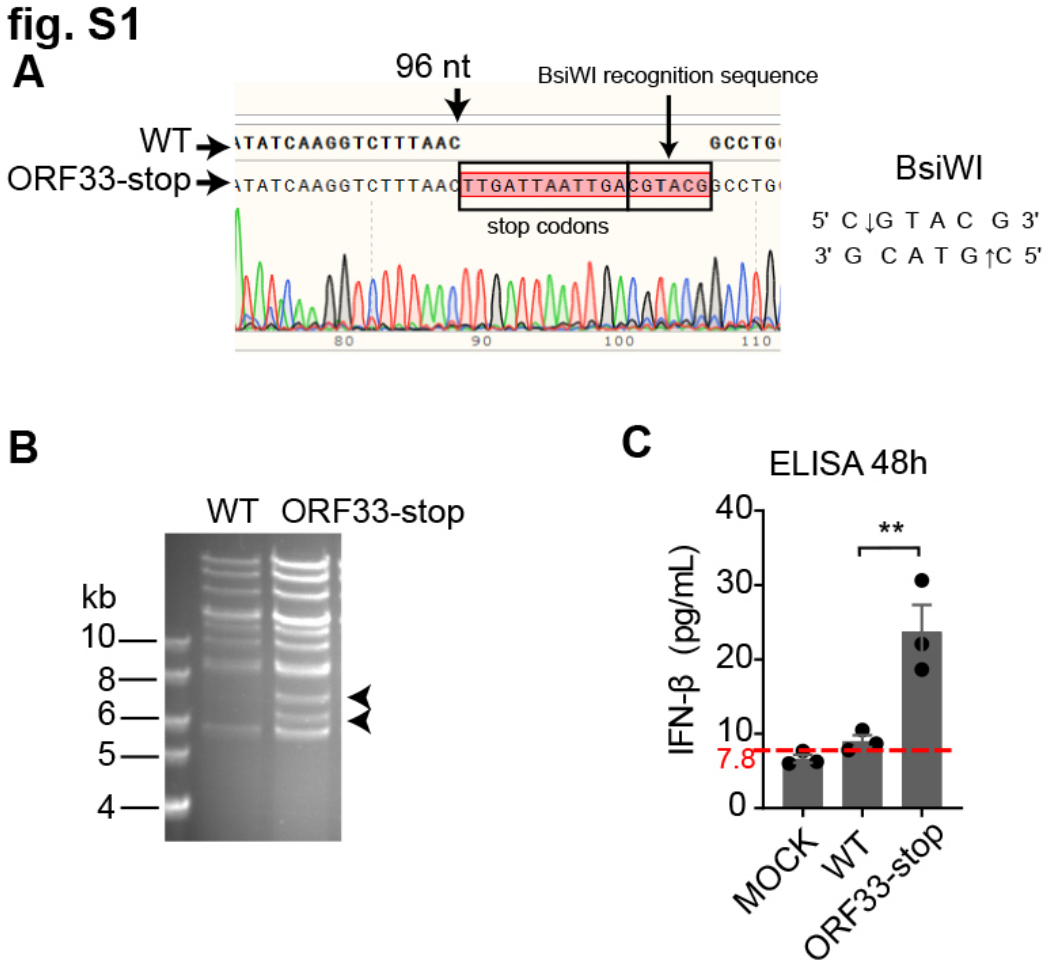

fig. S1. Construction and analysis of an ORF33-null KSHV BAC, Related to Fig. 1

(A) Nucleotide sequence of the region containing the mutation in the ORF33-null KSHV mutant BAC. A sequence fragment containing triple-frame translation termination codons and a *Bsi*WI restriction enzyme site (right panel) was inserted at 96 nt downstream of the translational initiation site of *ORF33* on KSHV RGB BAC16, to construct a ORF33-null RGB BAC16 (ORF33-stop).

(B) Analysis of WT or ORF33-null RGB BAC16 DNAs digested with *Bsi*WI by AGE (agarose gel electrophoresis). Arrowheads indicate the predicted differential DNA fragments resulting from insertion of the *Bsi*WI enzyme site into the ORF33-null BAC mutant.

(C) IFNβ levels in cell supernatant during reactivation of WT or ORF33-null mutant KSHV. iSLK cells latently infected with WT or ORF33-null KSHV were induced for 48 h. IFNβ levels in supernatant were measured by ELISA at 48 h post-treatment. The red dotted line indicates the lower limit of the assay range of IFNβ ELISA Kit.

(C) Data presented are means ± SEM of three independent measurements, representative of three independent experiments. **$p < 0.01$, Student's t test, $n = 3$.

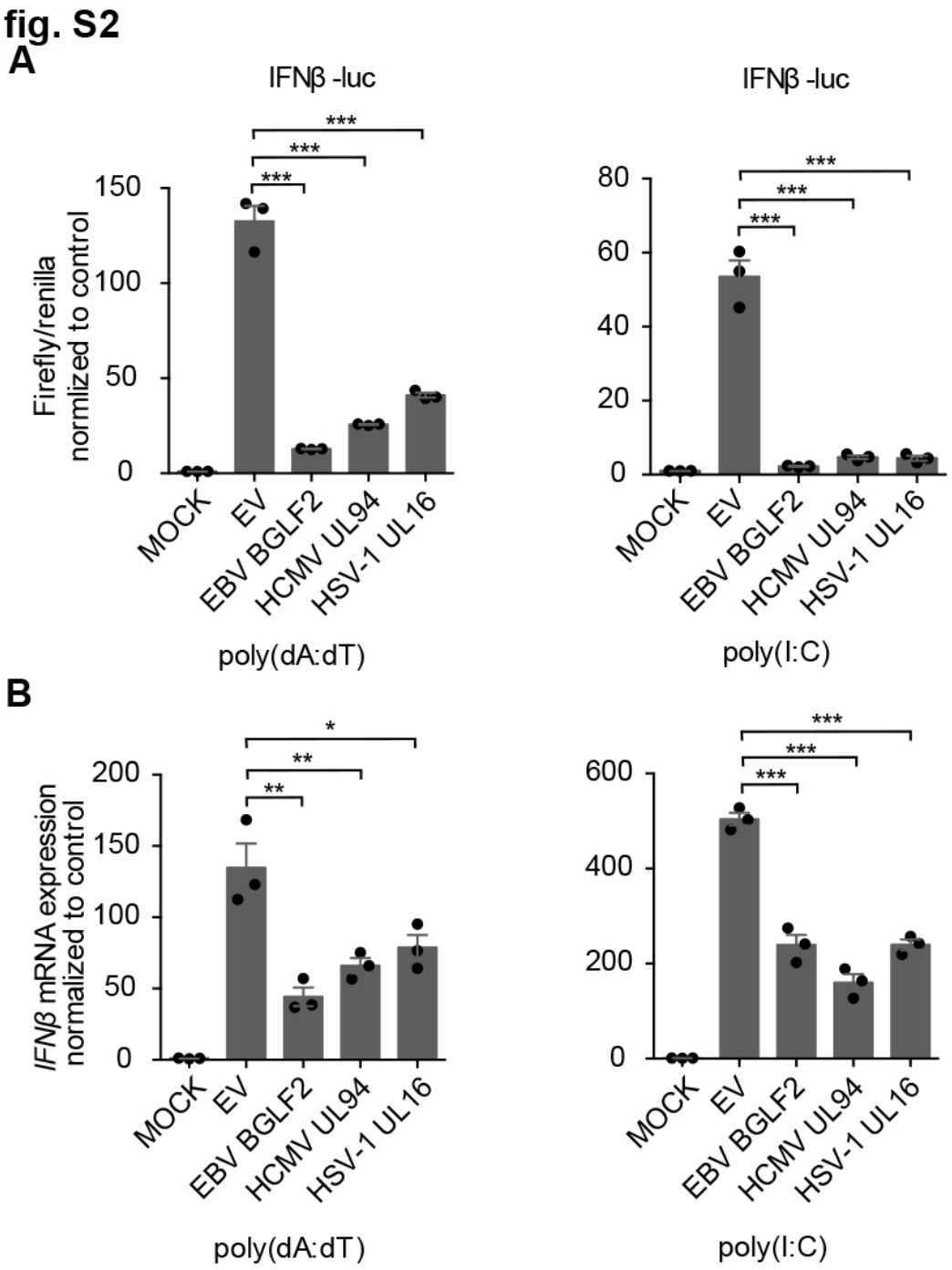

fig. S2. The homologues of ORF33 inhibit IFNβ production, Related to Fig. 1

(A) Influence of ORF33 homologues on *IFNβ*-luc indicator gene expression after poly(dA:dT) or poly(I:C) treatment. HEK293 cells were transfected with EV or individual expression plasmid for ORF33 homologues (EBV BGLF2, HCMV UL94 and HSV-1 UL16), along with IFNβ-luc reporter and TK-Renilla reporter plasmids for 24 h, treated with poly(dA:dT) or poly(I:C) for 18 h, and luciferase assays performed.

(B) Impact of ORF33 homologues on *IFNβ* mRNA levels after poly(dA:dT) or poly(I:C) treatment. HEK293 cells were transfected with EV or individual expression plasmid for ORF33 homologues (EBV BGLF2, HCMV UL94 and HSV-1 UL16) for 24 h, treated with poly(dA:dT) or poly(I:C) for 18 h, and *IFNβ* mRNA levels measured by RT-qPCR.

(A, B) Data presented are means ± SEM of three independent measurements, representative of three independent experiments. *$p < 0.05$, **$p < 0.01$ and ***$p < 0.001$; Student's t test, $n = 3$.

fig. S3

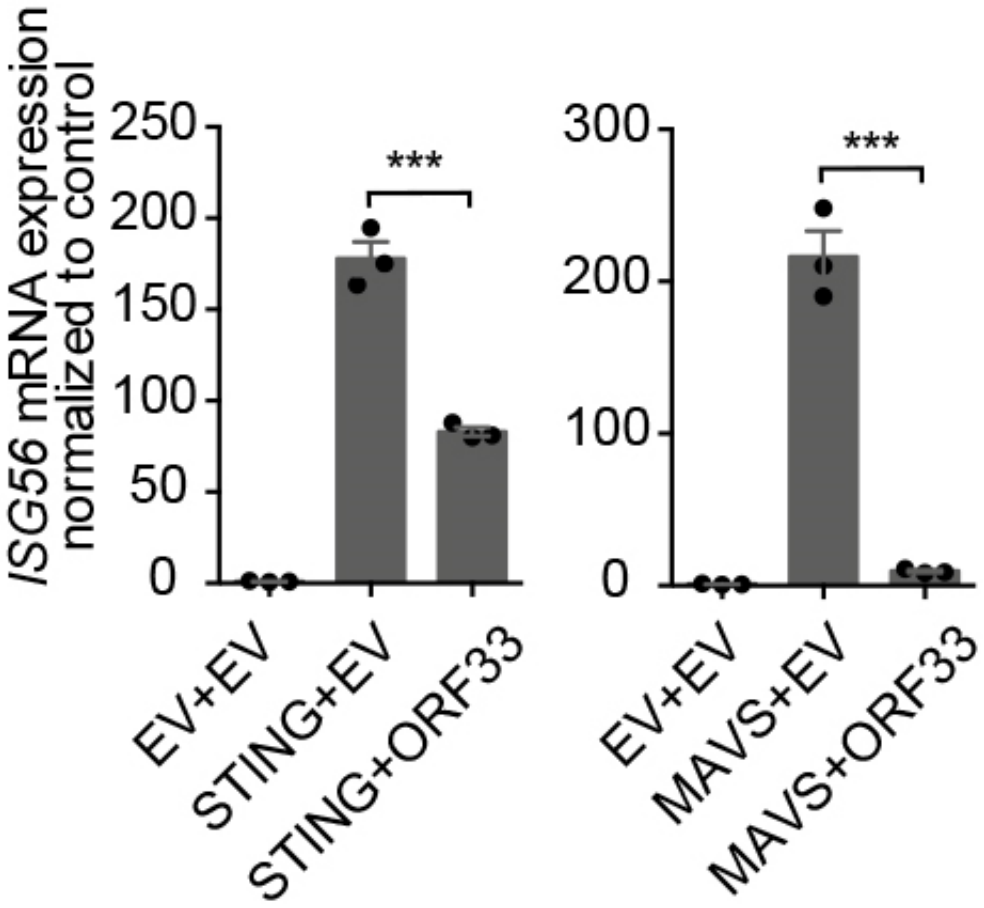

fig. S3. ORF33 inhibits the induction of Interferon-Stimulated Gene ISG56 expression by STING or MAVS, Related to Fig. 1

HEK293 cells were co-transfected with EV/KSHV ORF33 expression plasmid and STING (left)/MAVS (right) expression plasmid for 24 h. *ISG56* mRNA levels were measured by RT-qPCR. Data presented are means ± SEM of three independent measurements, representative of three independent experiments. ***$p < 0.001$, Student's t test, $n = 3$.

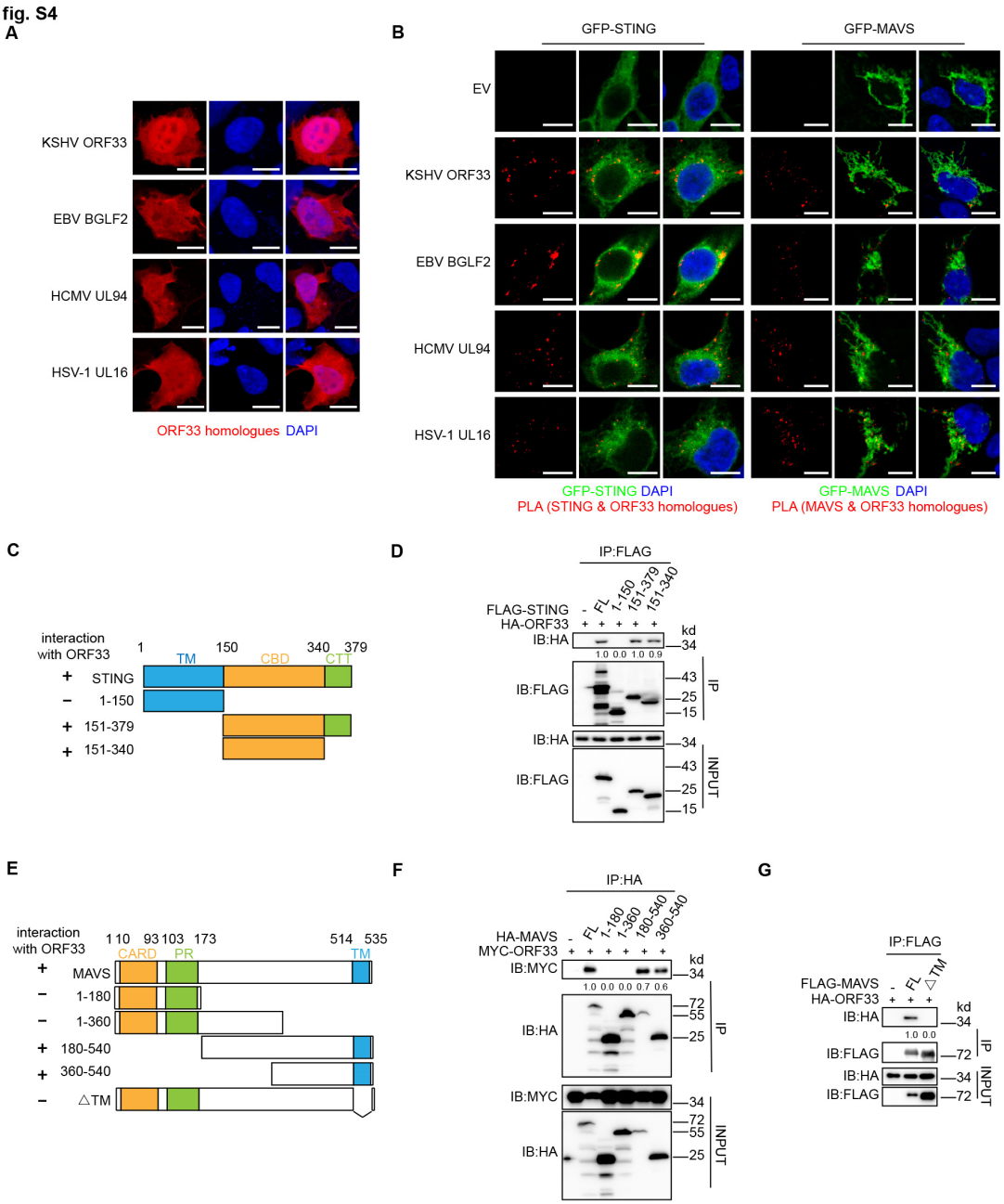

fig. S4. STING/MAVS interacts with ORF33 homologues, and the CBD domain of STING and TM domain of MAVS are required for ORF33 interaction, Related to Fig. 2

(**A**) The subcellular localizations of ORF33 homologues. HEK293 cells were individually transfected with HA-tagged expression plasmid for ORF33 homologues for 24 h. Cells were fixed and immunostained with anti-HA antibody. Scale bars, 10 μm.

(**B**) The interaction between ORF33 homologues and STING/MAVS. HEK293T cells were individually co-transfected with HA-tagged expression plasmid for ORF33 homologues and GFP-

STING/GFP-MAVS plasmid for 24 h. The anti-GFP and anti-HA antibodies were used for PLA. Scale bars, 10 μm.

(**C, D**) Domain mapping of the ORF33 and STING interaction. (C) A schematic graph showing the three structural domains of STING protein and the deletion constructs. (D) HEK293T cells were transfected with FLAG-STING (full length or truncated mutant) and HA-ORF33 expression plasmids for 36 h before coimmunoprecipitation. The gray values were quantified using Image J.

(**E-G**) Domain mapping of the ORF33 and MAVS interaction. (E) A schematic graph showing the three structural domains of MAVS protein and the deletion constructs. (F, G) HEK293T cells were transfected with HA-MAVS (full length or truncated mutant or TM-deleted mutant) and FLAG-ORF33 expression plasmids for 36 h before coimmunoprecipitation. The gray values were quantified using Image J.

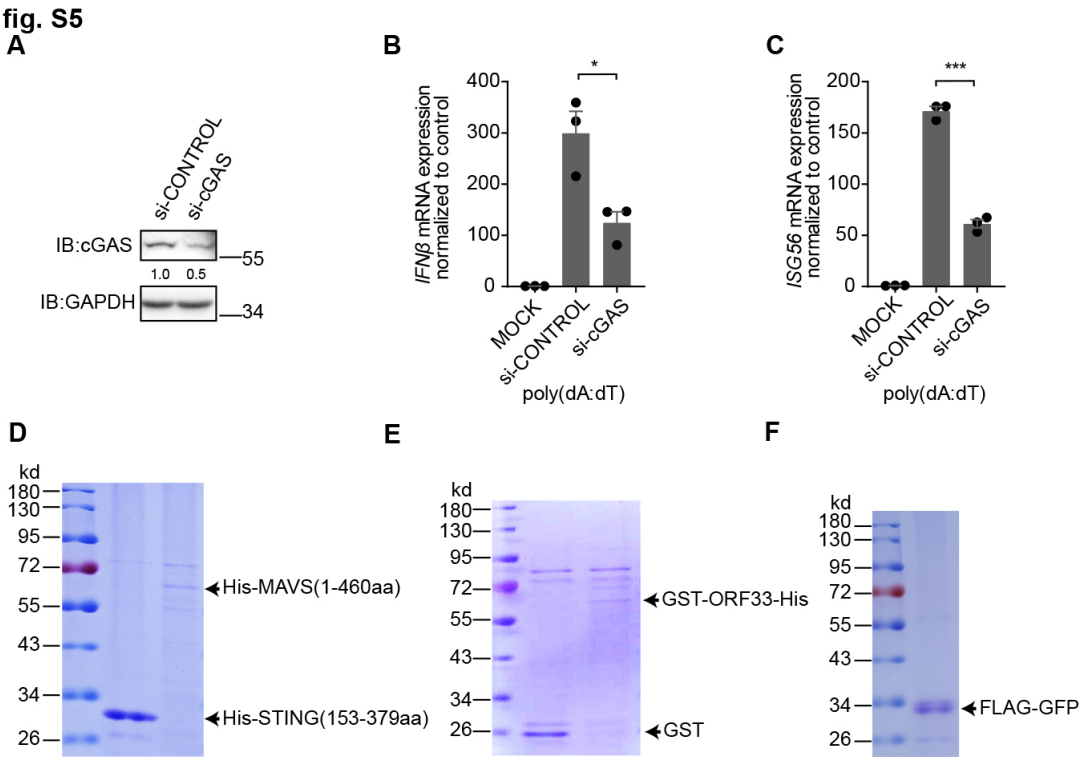

fig. S5. cGAS is expressed in HEK293 cells used in this study, Related to Fig. 3

(A) Immunoblotting analysis of the knockdown efficiency of *cGAS* by siRNA. HEK293 cells were transfected with siRNA for 48 h. The gray values were quantified using Image J and normalized to those of GAPDH.

(**B, C**) Influence of cGAS knockout on *IFNβ* and *ISG56* mRNA levels after poly(dA:dT) stimulation. After transfection with siRNA for 48 h, HEK293 cells were stimulated with poly(dA:dT) for 12 h. *IFNβ* and *ISG56* mRNA levels were measured by RT-qPCR.

(**D-F**) The coomassie blue stained gel of purified His-STING and His-MAVS from bacteria (D), purified GST and GST-ORF33-His from bacteria (E), purified FLAG-GFP from HEK293 cells (F).

(B, C) Data presented are means ± SEM of three independent measurements, representative of three independent experiments. *$p < 0.05$ and ***$p < 0.001$; Student's t test, $n = 3$.

fig. S6

A

Accession	Gene	Description	EV(Score)	ORF33(Score)
O00743	PPP6C	Serine/threonine protein phosphatase 6 catalytic subunit	0	38.46
P67775	PPP2CA	Serine/threonine protein phosphatase 2A catalytic subunit alpha	0	37.06
P62136	PPP1CA	Serine/threonine protein phosphatase PP1-alpha catalytic subunit	0	16.55
P62140	PPP1CB	Serine/threonine protein phosphatase PP1-beta catalytic subunit	0	12.45
O15355	PPM1G	protein phosphatase, Mg2+/Mn2+ dependent 1G	0	10.42
E9PPC8	PPP3CA	protein phosphatase 3 catalytic subunit alpha	0	4.01

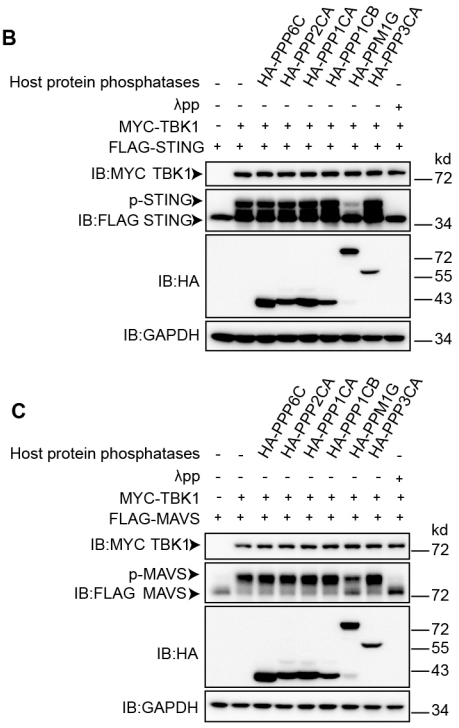

fig. S6. Identification of host protein phosphatases associated with ORF33 by IP-MS, Related to Fig. 4

(**A**) The host protein phosphatases associated with ORF33. HEK293 cells were transfected with EV or FLAG-ORF33 expression plasmid. After 36 h, cell lysates were incubated with anti-FLAG-M2 antibody-conjugated agarose for coimmunoprecipitation. Bound proteins were then eluted with 3×FLAG peptide and identified by mass spectrometry. Those protein phosphatases detected from ORF33 sample but not from the EV control sample were listed.

(**B, C**) The effect of host protein phosphatases on the phosphorylation levels of STING and MAVS. Experiment was performed as described in the legend to Fig. 3D.

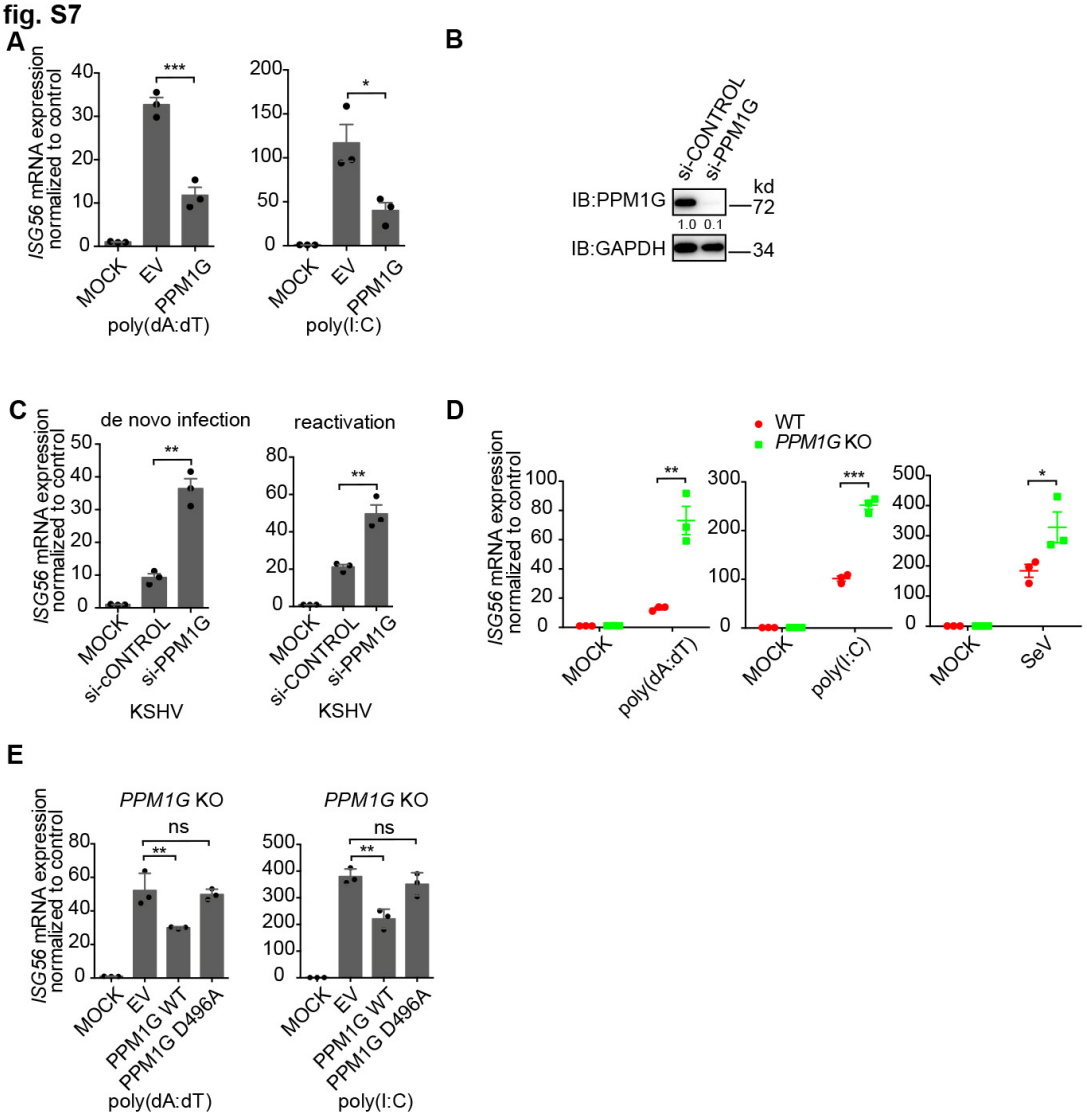

fig. S7. PPM1G inhibits the expression of interferon-stimulated gene ISG56, Related to Fig. 5

(A) Impact of PPM1G on *ISG56* mRNA levels. *ISG56* mRNA levels were measured by RT-qPCR, as described in the legend to Fig. 1C.

(B) Immunoblotting analysis of the knockdown efficiency of *PPM1G* by siRNA. The gray values were quantified using Image J and normalized to those of GAPDH.

(C) *ISG56* mRNA levels in control or PPM1G knockdown cells during de novo infection and reactivation of KSHV. *ISG56* mRNA levels were measured by RT-qPCR, as described in the legend to Fig. 5E.

(D) Influence of PPM1G knockout on *ISG56* mRNA levels. *ISG56* mRNA levels were measured by RT-qPCR.

(E) The phenotype exhibited by PPM1G knockout cells was reversed by introducing WT but not catalytically inactive (D496A) PPM1G mutant. *ISG56* mRNA levels were measured by RT-qPCR. (A), (C-E) Data presented are means ± SEM of three independent measurements, representative of three independent experiments. *$p < 0.05$, **$p < 0.01$, ***$p < 0.001$, ns, not significant; Student's t test, $n = 3$.

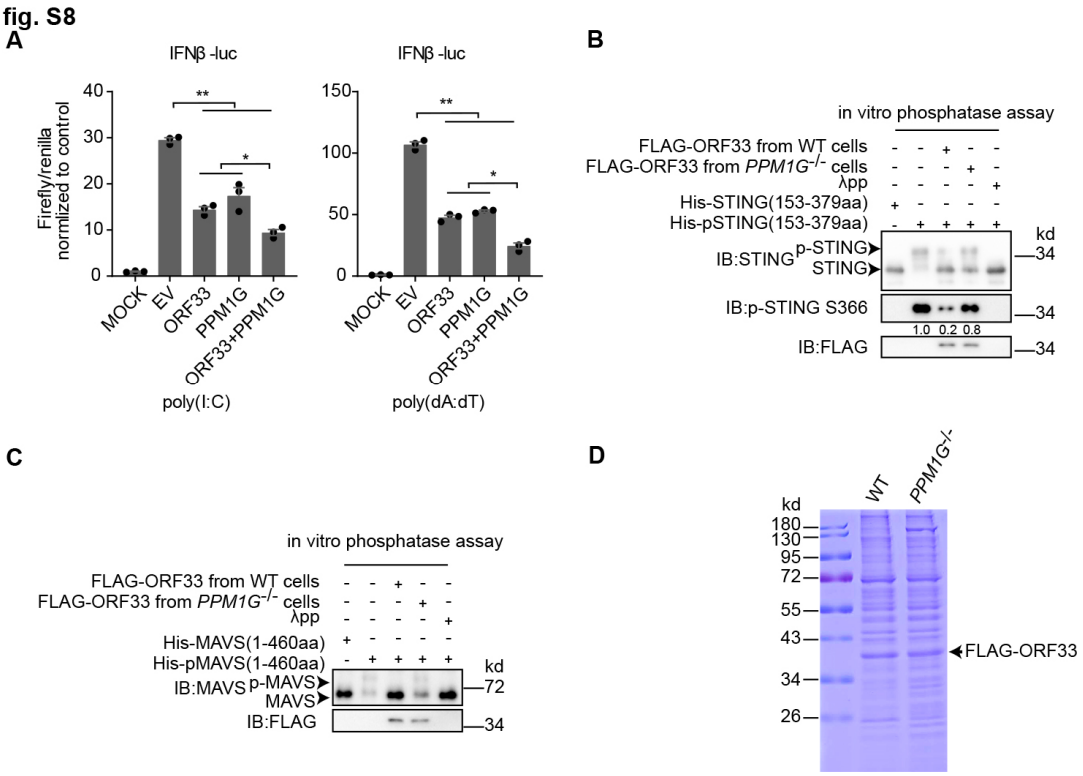

fig. S8. ORF33 relies on PPM1G to dephosphorylate p-STING and p-MAVS, Related to Fig. 7

(**A**) ORF33 and PPM1G synergistically reduced IFNβ-luc activity, as described in the legend to Fig.1B.

(**B, C**) The effect of FLAG-ORF33 extract from PPM1G KO cells on the phosphorylation of STING and MAVS, as described in the legend to Fig. 3, E and F.

(**D**) The coomassie blue stained gel of FLAG-ORF33 extract from WT/PPM1G KO cells.

(A) Data presented are means ± SEM of three independent measurements, representative of three independent experiments. *$p < 0.05$ and **$p < 0.01$; Student's t test, n = 3.

Table S1. Primer or oligo sequences (5'-3') used in this study

IFNβ-forward:	AAACTCATGAGCAGTCTGCA
IFNβ-reverse:	AGGAGATCTTCAGTTTCGGAGG
GAPDH-forward:	CGAGATCCCTCCAAAATCAA
GAPDH-reverse:	TTCACACCCATGACGAACAT
ISG56-forward:	ACGGCTGCCTAATTTACAGC
ISG56-reverse:	AGTGGCTGATATCTGGGTGC
ORF73-forward:	CGCGAATACCGCTATGTACTCA
ORF73-reverse	GGAACGCGCCTCATACGA
SeV NP-forward	CAAGAGCCCACTCTTCCAGGG
SeV NP-reverse	CTGAACGCCTCTAACCTGTTG
SeV M-forward	GTGATTTGGGCGGCATC
SeV M-reverse	GATGGCCGGTTGGAACAC
HSV-1 gD-forward	ACGACTGGACGGAGATTACA
HSV-1 gD-reverse	GGAGGGCGTACTTACAGGAG
HSV-1 gJ-forward	GGCCTGGCTATCCGGAGA
HSV-1 gJ-reverse	GCGCAGAGACATCGCGA
ORF33-stop-forward	GCATATGGACTGTTAACCCAATGTCAGGGGACCATATCAAGGT CTTTAACTTGATTAATTGACGTACGGCCTGCACCTCTATCTCGA CTGGTGTGACAAAGCC
ORF33-stop-reverse	TAGCTGGTTACCAGCTCAGGGTCATACACCGGCGAGATAGAG GTGCAGGCCGTACGTCAATTAATCAA
PPM1G-EXON1-top	CACCGCAACACGGTGAAGTGCTCCG
PPM1G-EXON1-bottom	AAACCGGAGCACTTCACCGTGTTGC
PPM1G-EXON9-top	CACCGTCGGTTATTGTCATCCATTG
PPM1G-EXON9-bottom	AAACCAATGGATGACAATAACCGAC